General mobility and carrier concentration relationship in transparent amorphous indium zinc oxide films

Andrew J. Leenheer,[1] John D. Perkins,[2] Maikel F. A. M. van Hest,[2] Joseph J. Berry,[2] Ryan P. O'Hayre,[1] and David S. Ginley[2,*]

[1]Department of Materials Science, Colorado School of Mines, 1800 Illinois St., Golden, Colorado 80401, USA

[2]National Renewable Energy Laboratory, 1617 Cole Boulevard, Golden, Colorado 80401, USA

(Received 24 December 2007; revised manuscript received 17 February 2008; published 28 March 2008)

We report the dependence of the electronic properties on the metal composition and oxygen content of transparent conducting amorphous indium zinc oxide (a-IZO) films deposited by dc magnetron sputtering. a-IZO shows a clear Burstein–Moss shift with an effective optical band gap of 3.1 eV independent of the metal composition. A metal-composition-independent dependence of the mobility (μ) on carrier concentration (N) is also found for a-IZO with $\mu_{max}=54$ cm^2/V s at $N=1.3\times10^{20}$ cm^{-3}. The electron transport, thermally activated at $N\leq10^{19}$ cm^{-3}, becomes limited by lattice scattering at $N\approx10^{20}$ cm^{-3} and then by ionized impurity scattering at $N>5\times10^{20}$ cm^{-3}.

DOI: 10.1103/PhysRevB.77.115215 PACS number(s): 73.50.−h, 73.61.Jc, 78.66.Jg

I. INTRODUCTION

Transparent conducting oxides (TCOs) are a special class of materials that combine high optical transparency due to a large intrinsic band gap (~3 eV) with tunable conductivity ranging from insulating to nearly metallic, typically arising from a defect or dopant-controlled n-type carrier concentration up to $>10^{21}$ cm^{-3}.[1] While traditional TCOs are highly crystalline, recently, a new class of amorphous TCO materials typified by amorphous In-Zn-O (a-IZO)[2–10] has emerged based on double (or triple) oxides of heavy metal cations with ionic electronic configuration $(n-1)d^{10}ns^0$.[11] These materials typically exhibit an unusually high electron mobility, $\mu\approx30-60$ cm^2/V s, which is thought to be due to a direct spatial overlap of the large and spherical heavy metal cation ns^0 orbitals, though recent first-principles calculations question this.[12] For comparison, typical thin film amorphous Si has mobilities of $\mu<1$ cm^2/V s.[13]

Smooth high-quality transparent conducting and semiconducting a-IZO thin films can be easily deposited onto a glass by sputtering at ambient temperature. Hence, these materials are of great technological interest for traditional TCO applications, such as flat panel displays and photovoltaics, as well as the new emerging area of transparent thin film transistors, an application requiring low-carrier concentration, semiconducting a-IZO as the channel layer.[14,15] However, for these new mixed metal oxide amorphous semiconductors, many fundamental questions remain, such as the electronic scattering mechanisms and the dependence of electronic properties on both composition and structure.

Optically and electronically, a-IZO appears to be quite similar to amorphous indium oxide (a-InO$_x$).[16,17] However, there appear to be several important differences. In particular, a-InO$_x$ quickly crystallizes into bixbyite In_2O_3 at modest temperatures, e.g., 20 min at 180 °C,[18] whereas a-IZO (depending on stoichiometry) does not crystallize until temperatures of >500 °C.[19] Furthermore, while a-InO$_x$ can only be grown over a relatively narrow range of deposition conditions,[20] a-IZO and similar amorphous mixed metal oxides can be deposited over a wide range of deposition conditions and metal compositions.[7,8,10,21] Practically, this has led to a-IZO being much more technologically important and the prototype amorphous TCO material. In addition, the properties of a-IZO can be measured over a much broader range of temperatures.

Here, we report on the effect of metals and oxygen composition on the electrical transport and optical properties of amorphous In-Zn-O. In particular, a-IZO thin films with metal compositions spanning the amorphous region (60/40 to 84/16 cation % In/Zn) were deposited at ambient temperature by dc magnetron sputtering in Ar containing 0–10% O_2. The effective optical band gap decreases to a floor at ~3.1 eV as the carrier concentration decreases, independent of the metal composition. Furthermore, and unexpectedly, for a-IZO we find a general metal-composition-independent relationship between the carrier concentration (N) and the mobility (μ) with a maximum room temperature mobility $\mu_{max}=54$ cm^2/V s at $N=1.3\times10^{20}$ cm^{-3}. At this maximum mobility, the mobility increases as the sample is cooled, which is indicative of lattice scattering, whereas at lower carrier concentration, $N\leq10^{19}$/cm^3, the electrical conduction is thermally activated and, at higher carrier concentration, $N>5\times10^{20}$/cm^3, ionized impurity scattering dominates.

II. EXPERIMENT

Indium zinc oxide films were deposited by magnetron sputtering on fused silica substrates ~1 cm^2 in area. Four 99.99% pure 2-in. (5.1 cm) diameter oxide In-Zn-O targets (most from Plasmaterials Inc.) were used to approximately span the amorphous range of IZO: 90/10, 87/13, 80/20 (Cerac, Inc.), and 72/28 wt. % In_2O_3/ZnO corresponding to 84/16, 80/20, 70/30, and 60/40 at. % In/Zn. An additional more Zn-rich target of 63/37 wt. % In_2O_3/ZnO (50/50 at. % In/Zn) resulted in crystalline films. Films were sputtered with a power density of 2.5 W/cm^2 and the target-to-substrate distance was ~11 cm. System base pressure was $<5\times10^{-6}$ Torr for all depositions. A shuttered burn-in was performed before each deposition with equal parts of oxygen

 ©2008 The American Physical Society

and argon gas for 7 min to ensure target stoichiometry,[5] followed by 3 min at the desired O_2 flow. During deposition, the pressure was held constant at 4.5 mTorr with a total gas flow of 10 SCCM (SCCM denotes cubic centimeter per minute at STP) composed of Ar with 0–10% O_2 by flow. The actual argon and oxygen partial pressures in the chamber were monitored with a residual gas monitor; both the % O_2 calculated by $100P_{O_2}/(P_{O_2}+P_{Ar})$ and the measured P_{O_2} are reported. The films were deposited at ambient temperature with no intentional substrate heating (substrate temperature <100 °C). The total deposition time was ~30 min, resulting in films 210–330 nm thick. After deposition, the amorphous film compositions were measured by inductively coupled plasma (ICP) analysis vs known standards and were found to be 86.0, 82.5, 76.3, and 64.5 at. % In with an uncertainty of ±5%, which is consistent with the nominally specified target composition. ICP also confirmed that the variation of metal composition as oxygen was added to the sputter gas was negligible. From here on, the compositions are designated by the at. % In present in the target.

Optical transmission and reflection spectra were taken for $\lambda=250-900$ nm using two Ocean Optics charge-coupled-device-based spectrometers, and film thickness was measured using a J. A. Woollam α-SE spectroscopic ellipsometer. Resistivity, carrier concentration, and Hall mobility were measured with an Accent HL5500 Hall-effect measurement system, which is equipped with a high-impedance picoampere current source and buffer amplifier, by contacting the corners of the films in the standard van der Pauw configuration. For the very resistive ($R_S > \sim 10^8\ \Omega/\square$) films deposited with $>5\%$ O_2 present in the sputtering gas, the Hall coefficient was not measurable. Structure was examined using x-ray diffraction (XRD) with a Bruker Discovery D8.

III. RESULTS AND DISCUSSION

A. Structure

Structure, as examined by XRD, was found to be amorphous for compositions ranging from 60 to 84 at. % In; a broad low-intensity hump evident at $2\theta \approx 33°$ with a full width at half maximum of 4° indicates that the materials are amorphous, which has been confirmed by transmission electron microscopy. Similar amorphous and/or microcrystalline XRD spectra have previously been seen for IZO.[2,5,22,23] However, the IZO films with 50 at. % In are crystalline as determined by XRD.

B. Optical properties

The optical transmission (T) and reflection (R) spectra for a typical film are shown in Fig. 1(a). Although interference oscillations are present due to the film thickness and an index of refraction mismatch between the film and the substrate, the film transmission normalized to the substrate is ~85% for visible light. In the ultraviolet, the band gap absorption reduces the transmission. The absorption coefficient (α) is calculated from R and T, and the optical band gap (E_{opt}) is determined by the Tauc relation $\alpha^x \propto (h\nu - E_{opt})$, where h is Planck's constant and ν is the photon frequency. For most

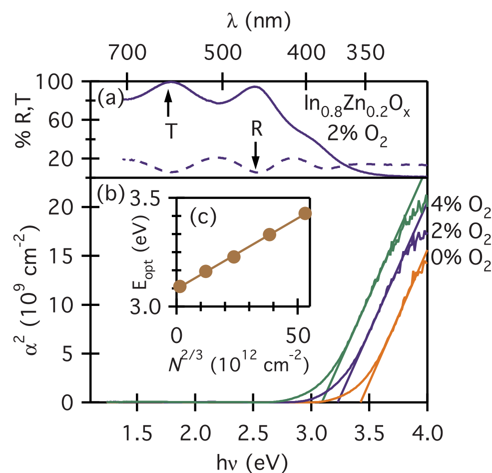

FIG. 1. (Color online) (a) Optical transmission, reflection, and (b) absorption coefficient versus photon energy for 80 at. % In films with 0, 2%, and 4% O_2. Absorption plot is fitted and the x intercept provides the optical band gap. (c) Optical band gap versus $N^{2/3}$.

amorphous semiconductors, nondirect optical transitions are allowed and the exponent x is $\frac{1}{2}$.[24] However, it has been reported that for amorphous indium oxide, electron momentum is largely conserved,[16] and the direct-band-gap model with $x=2$ provides a good description of an optical absorption band edge. Thus, α^2 is plotted versus photon energy in Fig. 1(b) for three different films, and the x intercept of a linear fit to the absorption data yields the optical band gap.[25] In all films, a sub-band-gap absorption tail is observed and attributed to the band tails in these amorphous materials.[25] The inset in Fig. 1(c) shows the decrease in band gap as the carrier concentration decreases. The linear trend of E_{opt} with $N^{2/3}$ is consistent with a Burstein–Moss shift for a three-dimensional parabolic band material.[26] The quality of the linear fit in the inset in Fig. 1(c) indicates that the conduction band states in these a-IZO materials appear to be well described by the parabolic band approximation for electron energies above the band tails. From the slope of the E_{opt} vs $N^{2/3}$ line, the combined effective mass ($1/m^*_{vc} = 1/m^*_v + 1/m^*_c$), which includes the effect of both valence and conduction band curvatures, is calculated to be $m^*_{vc} = 0.56 m_e$, where m_e is the electron rest mass.

Figure 2 provides the optical band gap data for all samples tested within the amorphous range. With increasing oxygen content in the sputtering gas, the band gap decreases to a floor, where the intrinsic band gap of approximately 3.1 eV is seen. Other studies have reported optical band gaps ranging from 3.5 to 3.9 eV for highly conductive films;[4,5,23] their high conductivity is correlated to a large Burstein–Moss shift away from our measured intrinsic gap at 3.1 eV. Collectively, for the data shown in Fig. 2, there is no clear systematic trend with the metal composition (at. % In). This indicates that the basic electronic structure is largely independent of the metal composition within the amorphous composition region (~55–85 at. % In) and that changes with varying oxygen content are significantly larger than any differences that may be due to the metal composition.

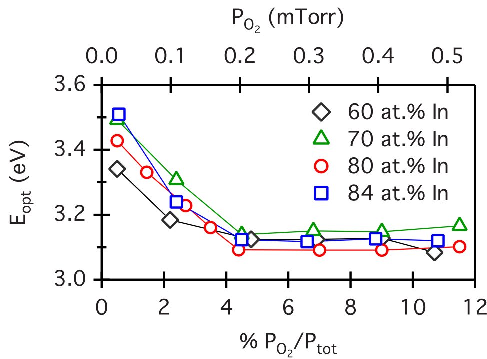

FIG. 2. (Color online) Optical band gap versus O_2 content in the sputtering gas for varying metal composition.

C. Electronic properties

Figure 3 shows the conductivity (σ) versus oxygen content for the *a*-IZO samples, as well as the carrier concentration and mobility on samples for which a good Hall measurement could be acquired. As expected, the conductivity and carrier concentration decrease by many orders of magnitude with increased oxygen content, though the mobility displays less of a clear pattern. By plotting the mobility versus the carrier concentration in Fig. 4(a), a clear trend emerges, which links μ to N for the amorphous IZO films. The carrier concentration is highest, $N \approx 5\times 10^{20}$ cm^{-3}, for samples deposited with no oxygen added to the argon sputter gas and decreases with oxygen addition down to $N \approx 10^{18}$ cm^{-3} at

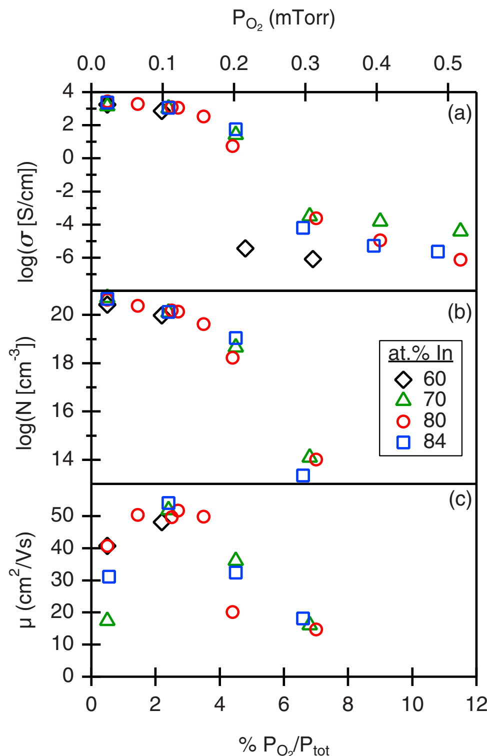

FIG. 3. (Color online) (a) Conductivity (σ), (b) carrier concentration (N), and (c) Hall mobility (μ) of the amorphous films versus oxygen content during sputtering.

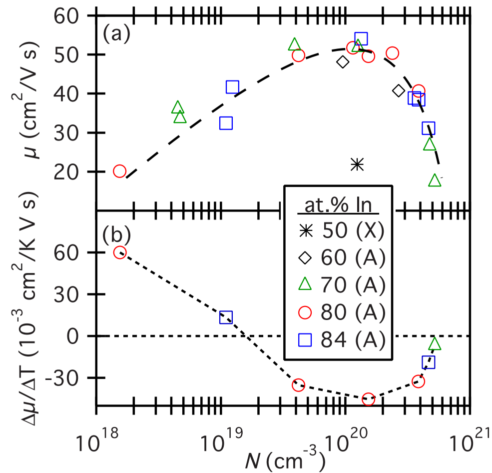

FIG. 4. (Color online) (a) Hall mobility (μ) versus carrier concentration (N) for amorphous and crystalline compositions denoted by A and X, respectively, with a dashed line included as a guide for the eye. (b) Slope of mobility versus temperature at various values of N.

~5% oxygen. The highest mobility of 54 cm^2/V s occurs when the carrier concentration is 1.3×10^{20} cm^{-3} and decreases on either side. Varying the metals-only ratio of In:Zn appears to have little effect on the relationship between N and μ, while the overall ratio In:Zn:O, and, especially, the oxygen stoichiometry, permits the adjustment of N to fall along the curve in Fig. 4(a) as long as the films remain in the amorphous regime. Note that the point for the crystalline 50 at. % In film (* in Fig. 4) does not fall on the general curve observed for the amorphous IZO films; thus, these results only hold for amorphous films.

This observed composition-independent trend indicates that the metal ratio in *a*-IZO is secondary to a more fundamental behavior related to the oxygen content. Furthermore, the curve seen in Fig. 4(a) suggests that different scattering mechanisms are limiting the mobility at different carrier concentrations. To reveal the plausible scattering mechanisms, temperature-dependent Hall measurements are shown in Fig. 5 with both cooling (closed symbols) and heating (open symbols) cycles. The temperature-dependent Hall measurements showed little temperature hysteresis, indicating that the samples have thermally equilibrated and are not physically changing during the measurement. The measured N was found to be independent of temperature and is noted for each sample in Fig. 5. At low carrier concentration, $N < 10^{19}$ cm^{-3}, the mobility decreases upon cooling ($\Delta\mu/\Delta T > 0$). At higher carrier concentrations, $N \geq 4\times 10^{19}$ cm^{-3}, the mobility increases as temperature decreases ($\Delta\mu/\Delta T < 0$) and, at the highest carrier concentrations, $N \approx 5\times 10^{20}$ cm^{-3}, the mobility becomes almost temperature independent ($\Delta\mu/\Delta T \to 0$).

To make this clearer, a linear fit for each trace in Fig. 5 provides an estimate for the temperature dependence of mobility, and the fit-determined slope $\Delta\mu/\Delta T$ is plotted in Fig. 4(b). For intermediate $N \geq 4\times 10^{19}$ cm^{-3}, $\Delta\mu/\Delta T < 0$, suggesting that lattice scattering, perhaps phonon or alloy related, limits the mobility.[27] Then, at very high carrier con-

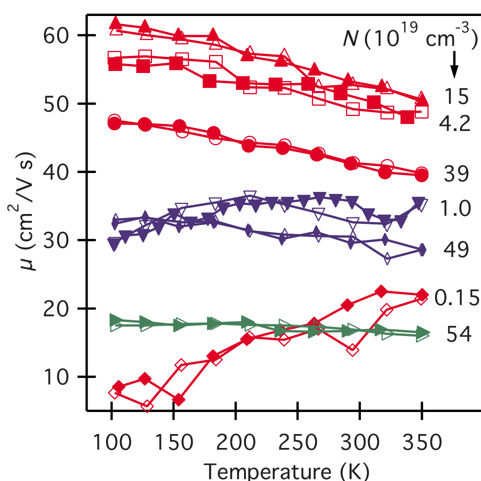

FIG. 5. (Color online) Hall mobility versus temperature for which both heating (open symbols) and cooling (closed symbols) cycles are shown. Carrier concentration (N) indicated for each trace.

centration, $N \approx 5 \times 10^{20}$ cm^{-3}, the mobility varies only slightly with temperature, suggesting a highly degenerate ionized impurity type scattering.[26] In contrast, at low carrier concentration ($N = 1.5 \times 10^{18}$ cm^{-3}), $\Delta\mu/\Delta T > 0$ and the measured conductivity is thermally activated and well described by a hopping or percolation model.[26,28] The "floor" in the conductivity at high O_2 content ($<5\%$) also indicates hopping or percolation conductivity. We note that the peak in mobility occurs where the mobility-temperature slope is the most negative, as seen in Fig. 4. Therefore, the highest mobility occurs when the intrinsic lattice scattering is the limiting factor and the temperature dependence of the conduction is essentially metallic.

Similar results have been reported for *a*-IZO[7,8] and *a*-InO_x.[17] For *a*-IZO films (84 at.% In) deposited at room temperature by rf magnetron sputtering in varying amounts of oxygen, Martins *et al.*[8] observed a monotonic increase of μ with increasing N, yielding $\mu_{max} \approx 60$ cm^2/V s at $N \approx 4 \times 10^{20}$ cm^{-3}. For *a*-IZO films in the range 57–81 at.% In deposited at 200 °C by dc magnetron sputtering in pure Ar, Kumar *et al.*[7] observed an increase in mobility with increasing indium content, resulting in $\mu_{max} \approx 71$ cm^2/V s at $N \approx 2 \times 10^{20}$ cm^{-3} for the 81 at. % In *a*-IZO film. For *a*-InO_x films containing no zinc, Nakazawa *et al.*[17] observed an increasing mobility with increasing carrier concentration up to $\mu_{max} \approx 60$ cm^2/V s at $N \approx 2.5 \times 10^{20}$ cm^{-3} with a subsequent decrease in the mobility at higher carrier concentrations. While these results do not lie exactly along the general μ-N curve we show in Fig. 4 for *a*-IZO films grown at room temperature by dc magnetron sputtering, taken as a whole they are remarkably similar, given the different compositions, deposition techniques, and deposition temperatures involved. Finally, we note that for an amorphous In-Ga-Zn-O with a nominal 1:1:1 metal composition, Takagi *et al.* observed a mobility increase with increasing carrier concentration similar to what is observed for *a*-IZO, but the maximum mobility is lower, $\mu_{max} \approx 13$ cm^2/V s at $N \approx 10^{20}$ cm^{-3},[21] in this ternary mixed metal oxide material.

For amorphous mixed metal oxides such as *a*-IZO where the carrier concentration can vary by several orders of magnitude, the existence of different scattering mechanisms as a function of the carrier concentration is not unexpected and has been observed in the literature. At high N, E_F is well into the conduction band and the optical band gap is large [Fig. 1(c)]. At the highest $N (>5 \times 10^{20}$ cm$^{-3})$, a large number of oxygen-vacancy-like electron-donating defects are likely present, and degenerate ionized impurity scattering is more dominant. Ito *et al.*[4] found a similar behavior for 83 at. % In *a*-IZO films sputtered in a reducing atmosphere to obtain $N > 10^{20}$ cm^{-3} IZO, and the decrease of μ with increasing N was attributed to ionized impurity scattering along with some neutral and electron scattering.[4] Ionized impurity scattering is also known to be important for traditional high-N TCOs, such as indium oxide or indium tin oxide.[26] At $N \approx 10^{20}$ cm^{-3}, scattering is likely due mostly to vibrations and disorder for these IZO films; alternatively, scattering by charged structural or surface defects as N decreases has been proposed by Martins *et al.*[8] Below $N \approx 10^{19}$ cm^{-3}, the conduction electrons are likely trapped in localized states and the conductivity is therefore controlled by a hopping or percolation process as is frequently observed in amorphous materials.[26] Martins *et al.* also reported percolation conduction for IZO films sputtered in the presence of oxygen.[23] Nomura *et al.*[28] studied the In-Ga-Zn-O system at length, in which Ga is added to further reduce the carrier concentration. For single-crystalline $InGaO_3(ZnO)_5$, they found a similar dependence of mobility on N in the range 10^{17}–10^{19} cm^{-3} and attributed the trend to percolation conduction between tail states when the Fermi energy is less than a threshold energy, where the films become degenerate. Hosono[11] and Nomura *et al.*[29] also reported results for amorphous IZO and amorphous In-Ga-Zn-O, suggesting that percolation conduction switches to degenerate conduction mechanisms as N is increased. Here, our results show multiple transitions in the conduction mechanism with increasing N: first, from temperature-activated conduction to conduction limited by lattice scattering, and then at higher N degenerate ionized impurity scattering. In addition, this study provides observations of a metal-composition-independent relation between N and μ for an amorphous transparent conducting oxide.

From these results, as most clearly seen in Fig. 4, it appears that the Zn-related electronic states likely have only a weak effect on the overall band structure or are very similar to In-related states. This has been discussed in recent first-principles calculations by Medvedeva, who found that In, Zn, and O states significantly contribute to the conduction band and, for practical purposes, that the electron effective mass in these amorphous mixed metal oxide systems is reasonably approximated by averaging the effective masses of the constituent simple metal oxides.[12] In this light, previous work in which only either the metal composition[7,9,10] or the oxygen pressure during deposition[8,21] was varied can be understood as one-dimensional slices in a coupled two-dimensional parameter space, where the carrier concentration depends on both the metal composition and the oxygen present during deposition, and the mobility depends on the carrier concentration.

IV. SUMMARY

In summary, the transparent semiconducting *a*-IZO in the 60–84 at. % In range is found to display an intrinsic band gap of $E_{opt} \approx 3.1$ eV independent of the specific metal composition and a clear Burstein–Moss shift in the most conductive films. A general relationship between carrier concentration and mobility for these amorphous TCO films is found, again independent of the metal composition. The mobility appears to depend primarily on the carrier concentration, and N can be tuned primarily by the oxygen content in the sputtering gas with a small dependence on the metal ratio In:Zn. As the carrier concentration (N) increases, the conduction is initially thermally activated at $N \leqslant 10^{19}$ cm^{-3}, transitioning to lattice scattering at $N \approx 10^{20}$ cm^{-3} and ionized impurity scattering at $N > 5 \times 10^{20}$ cm^{-3}. This result may also apply to other transparent conducting amorphous mixed metal oxides that are dominated by *s*-band conduction. These results provide important insights into the basic electron transport properties of *a*-IZO and will also be of great value in optimizing *a*-IZO for any specific application.

ACKNOWLEDGMENTS

This work was supported by the National Center for Photovoltaics (NCPV), NREL's Laboratory Directed Research and Development (LDRD) in the transparent conducting oxide program, and the Air Force Research Laboratories (AFRL).

*Corresponding author; david_ginley@nrel.gov

[1] D. S. Ginley and C. Bright, MRS Bull. **25**, 15 (2000).
[2] E. Fortunato, A. Pimentel, A. Gonçalves, A. Marques, and R. Martins, Thin Solid Films **502**, 104 (2006).
[3] H. Hara, T. Hanada, T. Shiro, and T. Yatabe, J. Vac. Sci. Technol. A **22**, 1726 (2004).
[4] N. Ito, Y. Sato, P. K. Song, A. Kaijio, K. Inoue, and Y. Shigesato, Thin Solid Films **496**, 99 (2005).
[5] H.-C. Pan, M.-H. Shiao, C.-Y. Su, and C.-N. Hsiao, J. Vac. Sci. Technol. A **23**, 1187 (2005).
[6] B. Yaglioglu, Y.-J. Huang, H.-Y. Yeom, and D. C. Paine, Thin Solid Films **496**, 89 (2006).
[7] B. Kumar, H. Gong, and R. Akkipeddi, J. Appl. Phys. **98**, 073703 (2005).
[8] R. Martins, P. Barquinha, A. Pimentel, L. Pereira, and E. Fortunato, Phys. Status Solidi A **202**, R95 (2005).
[9] T. Minami, J. Vac. Sci. Technol. A **17**, 1765 (1999).
[10] M. P. Taylor, D. W. Readey, C. W. Teplin, M. F. A. M. van Hest, J. L. Alleman, M. S. Dabney, L. M. Gedvilas, B. M. Keyes, B. To, J. D. Perkins, and D. S. Ginley, Meas. Sci. Technol. **16**, 90 (2005).
[11] H. Hosono, J. Non-Cryst. Solids **352**, 851 (2006).
[12] J. E. Medvedeva, EPL **78**, 57004 (2007).
[13] H. Hosono, M. Yasukawa, and H. Kawazoe, J. Non-Cryst. Solids **203**, 334 (1996).
[14] N. L. Dehuff, E. S. Kettenring, D. Hong, H. Q. Chiang, J. F. Wager, R. L. Hoffman, C.-H. Park, and D. A. Keszler, J. Appl. Phys. **97**, 064505 (2005).
[15] B. Yaglioglu, H. Y. Yeom, R. Beresford, and D. C. Paine, Appl. Phys. Lett. **89**, 062103 (2006).
[16] J. R. Bellingham, W. A. Phillips, and C. J. Adkins, J. Phys.: Condens. Matter **2**, 6207 (1990).
[17] H. Nakazawa, Y. Ito, E. Matsumoto, K. Adachi, N. Aoki, and Y. Ochiai, J. Appl. Phys. **100**, 093706 (2006).
[18] Y. Shigesato and D. C. Paine, Appl. Phys. Lett. **62**, 1268 (1993).
[19] B. Yaglioglu, H. Y. Yeom, and D. C. Paine, Appl. Phys. Lett. **86**, 261908 (2005).
[20] J. R. Bellingham, W. A. Phillips, and C. J. Adkins, Thin Solid Films **195**, 23 (1991).
[21] A. Takagi, K. Nomura, H. Ohta, H. Yanagi, T. Kamiya, M. Hirano, and H. Hosono, Thin Solid Films **486**, 38 (2005).
[22] D. Y. Ku, I. H. Kim, I. Lee, K. S. Lee, T. S. Lee, J.-h. Jeong, B. Cheong, Y.-J. Baik, and W. M. Kim, Thin Solid Films **515**, 1364 (2006).
[23] R. Martins, P. Almeida, P. Barquinha, L. Pereira, A. Pimentel, I. Ferriera, and E. Fortunato, J. Non-Cryst. Solids **352**, 1471 (2006).
[24] N. F. Mott and E. A. Davis, *Electronic Processes in Non-Crystalline Materials* (Oxford University Press, Oxford, 1979).
[25] J. I. Pankove, *Optical Processes in Semiconductors* (Dover, New York, 1971).
[26] H. L. Hartnagel, A. L. Dawar, A. K. Jain, and C. Jagadish, *Semiconducting Transparent Thin Films* (Institute of Physics, Bristol, 1995).
[27] B. R. Nag, *Electron Transport in Compound Semiconductors* (Springer-Verlag, Berlin, 1980).
[28] K. Nomura, T. Kamiya, H. Ohta, K. Ueda, M. Hirano, and H. Hosono, Appl. Phys. Lett. **85**, 1993 (2004).
[29] K. Nomura, A. Takagi, T. Kamiya, H. Ohta, M. Hirano, and H. Hosono, Jpn. J. Appl. Phys., Part 1 **45**, 4303 (2006).